In-Orbit Performance of the ISO Short-Wavelength Spectrometer

Th. de Graauw[a,h], H. Feuchtgruber[b,c], P.R. Roelfsema[a], A. Salama[c], O. Bauer[b], D. Beintema[a], D. Boxhoorn[a,c], L. Decin[d], L. Haser[b], A. Heras[c], R. Huygen[d], R. Katterloher[b], D. Kester[a], D. Kunze[b], F. Lahuis[a,c], K. Leech[c], C. Lorente[c], D. Lutz[b], P. Morris[c,e], , S. Schaeidt[b], E. Sturm[b], E. Valentijn[a,c], B. Vandenbussche[c,d], R. Waters[f], E. Wieprecht[b,c], E. Wiezorrek[b], E. Young[g].

[a]SRON-Groningen, P.O.Box 800, 9700 AV Groningen, the Netherlands
[b]Max-Planck-Institute fur Extraterrestrische Physik, Postfach 1603, D-85740 Garching, Germany
[c]ISO Science Operations Center, Post-box 50727, E-28080Villafranca/Madrid, Spain
[d]Instituut voor Sterrenkunde, Univ. van Leuven, Celestijnenlaan 200B, 3001 Heverlee, Belgium
[e]SRON-Utrecht, Sorbonnelaan 2, 3584 CA Utrecht, the Netherlands
[f]Astron. Institute Anton Pannekoek, Univ.of Amsterdam, Kruislaan 403, 1098 SJ Amsterdam, the Netherlands
[g]Steward Observatory, University of Arizona, Tucson, USA
[h]Kapteyn Astronomical Institute, P.O.Box 800, 9700 AV Groningen, the Netherlands

ABSTRACT

The Short-Wavelength Spectrometer (SWS) is one of the four instruments on-board of ESA's Infrared Space Observatory (ISO), launched on 15 Nov. 1995. It covers the wavelength range of 2.38-45.2 microns with a spectral resolution ranging from 1000-2000. By inserting Fabry-Perot filters the resolution can be enhanced by a factor 20 for the wavelength range from 11.4-44.5 microns. After the successful launch the instrument was tested and calibrated during a period of spacecraft checkout and performance verification. The opto-mechanical construction of the instrument appears to behave extremely well. The instrument performance is on all aspects as expected, except for the detector sensitivity where the noise is dominated by effects of particle radiation. We give here an overview of the in-orbit performance, discuss the calibration and present some results from trend analysis of the most important instrument and detector parameters.

1. INTRODUCTION

The SWS is one of the two spectrometers on-board of ISO. Together with the Long-Wavelength Spectrometer it provides ISO with unprecedented capabilities for moderate and high spectral resolution observations, from the near to far infrared, altogether over 6 octaves.

The SWS covers, with its two grating sections, the wavelength range from 2.38-45.2 microns with a spectral resolving power of the order of 1000-2500. Using also the Fabry-Perot (F-P) etalons, which are located at the output of the long-wavelength (LW) grating section, the resolution can be increased above 25,000 for the wavelength range from 11.4-44.5 microns.

The SWS instrument was developed, fabricated and space-qualified by SRON and MPE, with contributions by the Steward Observatory and by the AGL Phillips Laboratory, Hanscom, USA. More details on the design of the SWS can be found in de Graauw[1] et al. and on the mechanisms in Wildeman[2] et al.

A team of software engineers and scientists supplied by SRON, MPE and ESA carried out the preparation and operation of the SWS. Home teams in Groningen, Garching and Leuven also supported the SWS instrument dedicated team (SIDT) in Vilspa. After the successful launch on 15 November 1995, there was a period of three weeks of spacecraft- and instrument checkout followed by 8 weeks of performance verification (PV) and calibration observations. These measurements and observations led to a preliminary in-orbit flux calibration and beam profile determination (Schaeidt[3] et al.), together with the first Relative Spectral Response Function (RSRF). For the results of the first in-orbit wavelength calibration, spectral resolution and instrumental profiles, see Valentijn[4] et al.

Part of the SPIE Conference on Infrared Astronomical Instrumentation • Kona, Hawaii • March 1998
SPIE Vol. 3354 • 0277-786X/98/$10.00

We first will give here a short description of the instrument followed by an overview of the so-called Astronomical Observing Templates (AOT) of SWS and their in-orbit performance. These AOT's are the building blocks of the observations to be carried out with ISO and the interface with the observer. Although the ISO satellite has uninterrupted ground contact during observations, almost all observations are pre-planned and AOT's have played an important role in reaching the high observing efficiency (>90%). We give a detailed account of the hardware performance where in particular the detector behaviour in the environment of cosmic radiation particles is addressed. We conclude with a summary of the status quo of the calibration.

2. INSTRUMENT DESCRIPTION

The SWS instrument consists of two nearly independent grating spectrometers plus a set of two scanning Fabry-Perot filters. See figure 1. The short wavelength section (SW) uses a 100-lines/mm grating in the first four orders covering 2.3-12.0 microns. The long wavelength (LW) section has a 30-lines/mm grating in the first two orders covering 11-45 microns. The two FP's are at the output of the LW section and use the first three orders of the LW grating. The SWS has three apertures and a shutter system allows to use only one of them while keeping the other two closed. For observations the spacecraft pointing has to be adjusted to have the astronomical object imaged onto the selected aperture. Each aperture is used for two wavelength ranges, one for the SW section and one for the LW section. This is achieved by using Reststrahlen crystal filters as wavelength selective beamsplitters behind the apertures. The transmitted beams are entering the SW section; the reflected beams enter the LW section. The actual spectrometer slits are located behind the beamsplitting crystals. Interference filters or crystal filters take care of further order sorting. Each grating has its own scanning device, allowing the use of both grating sections of the SWS at the same time, albeit through the same aperture. The scanning device consists of a rotating flat mirror supported by two flexural pivots and its driving force comes from a moving coil in a radial-oriented magnetic field. The position readout is with a LVDT. The output of each of the two grating sections is re-imaged onto two small (1*12) detector arrays, located in-line. The types of detectors in use, are listed in table I. The detector read-out is done with an integrating amplifier and signal level is derived from slope determination of the integration ramps.

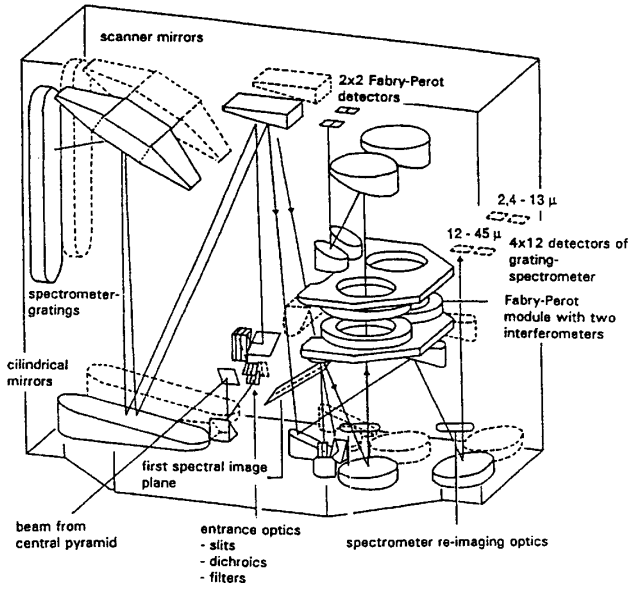

Figure 1. Schematic layout of the ISO-Short-Wavelength Spectrometer

Table 1 gives also an overview of the wavelength ranges for the various grating sections and orders, apertures and slit sizes and detector bands, resulting in the 12 so-called AOT bands. These bands play an important role in the data reduction and analysis, since a full SWS spectrum is composed out of 12 sub-spectra from these bands.

The scanning mechanism is also used to select the wavelengths for the two scanning FP's, as their inputs are located at the exit of the LW section. The FP's are mounted on a single pair of parallel plates, whose separation can be varied by changing the currents in three coils, thus scanning the wavelength. Scanning is performed according to two on-board calibration tables, one for each F-P. These tables are determined from calibration observations of narrow emission lines. There are 5 FP AOT bands, see again table 1.
The Relative Spectral Response Function (RSFR) of the instrument was determined on the ground using a black body source.

Table 1. Overview of the SWS AOT bands together with the in-orbit/ground sensitivity ratios, flux calibration accuracy and reproducibility

	Band	λ *key* (μm)	Grating order	Aperture Nr.	Area (")	Detector Type	pixels	Wavelength range	Sensitivity In-orbit / Ground	Flux Cal Accuracy %
SW Section	1A	2.5	SW4	1	14 x 20	InSb	1 x 12	2.38 - 2.60	0.6	5
	1B	2.9	SW3	1	14 x 20	InSb	1 x 12	2.60 - 3.02	0.6	5
	1D	3.1	SW3	2	14 x 20	InSb	1 x 12	3.02 - 3.52	1.1	5
	1E	3.8	SW2	2	14 x 20	InSb	1 x 12	3.52 - 4.08	1.1	5
	2A	4.5	SW2	2	14 x 20	Si:Ga	1 x 12	4.08 - 5.30	4.5	7
	2B	5.9	SW1	2	14 x 20	Si:Ga	1 x 12	5.30 - 7.00	4.5	7
	2C	7.7	SW1	3	14 x 20	Si :Ga	1 x 12	7.00 - 12.00	4.5	11
LW Section	3A	14.0	LW2	1	14 x 27	Si :As	1 x 12	12.0 - 16.5	6.5	11
	3C	17.0	LW2	2	14 x 27	Si :As	1 x 12	16.5 - 19.5	6.5	11
	3D	24.0	LW1	2	14 x 27	Si:As	1 x 12	19.5 - 27.5	6.5	12
	3E	28.5	LW1	3	20 x 27	Si :As	1 x 12	27.5 - 29.0	6.5	20
	4	32.0	LW1	3	20 x 33	Ge:Be	1 x12	29.0 - 45.2	5.5	30
F-P	5A	11.8	LW3	1	10 x 39	Si:Sb	1 x 2	11.4 - 12.2	5.5	
	5B	14.0	LW2	1	10 x 39	Si:S	1 x 2	12.2 - 16.0	1.7	
	5C	17.0	LW2	2	10 x 39	Si:Sb	1 x 2	16.0 - 19.0	1.7	
	5D	24.0	LW1	2	10 x 39	Si:Sb	1 x 2	19.0 - 26.0	2.0	
	6	27.0	LW1	3	17 x 40	Ge:Be	1 x 2	26.0 - 44.5	2.1	

3. SWS OBSERVING MODES AND AOT'S

There are two main SWS observing modes: observing with the two SWS grating sections and with the Fabry-Perot/SW grating section combination.
In the grating observations the spectral ranges (for both sections) are directed to the designated arrays of 1*12 detectors. The spectral range covered instantaneously is of the order of 8 resolution elements. The gratings are scanned in steps with different step schemes depending on the AOT used. These schemes are optimised for line observations (AOT-02), for scans of wavelength ranges (AOT-06) and also for full SWS wavelength range scans (AOT-01) with different speeds (/1, /2, /3, /4) and respective resolving powers (200, 400, 800. 1600).
For the FP observations AOT-07 is used. Here the LW grating section is used as order sorter with the maximum of the grating transmission tuned to the desired wavelength. When scanning the FP, tracking for optimum grating transmission is needed to maximise the transmission and to minimise the contribution of unwanted FP orders. Parallel to the FP scans, the SW section can be used for grating spectral range observations. There are no SWS-dedicated spatial raster AOT's. Mapping is to be accomplished by successive pointing.

After launch, the AOT's were extensively tested since they were also used for most of the calibration observations. Only relatively small adjustments had to be made, mainly to cope with impacts of the ionising particles. Because of the high frequency of the impacts, the integration ramps had to be limited to 2 seconds, except for band 1 where 4 seconds is also possible. The dark current measurements were optimised; the duration and occurrence was extended. Because of the stability of the SWS instrument in orbit, the responsivity check at the start of an observation could be deleted and in other cases minimised. The high-level responsivity checks, introduced to check the band 1 detectors, were totally abandoned. These responsivity checks were a major disturbance for band 1, 2, 4, 5, and 6.
The suspicion that band 3D had a second-order leakage problem between 27.5 and 28 micron was confirmed and band 3E was

extended downward to include this wavelength range. Some unnecessary large overlaps between the bands could be eliminated. Reference scans, designed to improve determination of responsivity, together with memory effects can, in the case of a strong signal at the reference wavelength, affect the flux calibration in the subsequent observations. Although this effect can only occur in band 2 and 4, and only if the reference scan signal is many times higher than the average signal, it was finally decided to eliminate the reference scans altogether.

4. IN-ORBIT HARDWARE PERFORMANCE

In-orbit, the SWS instrument appeared to be very stable. As the ground calibration and tests did not include measurements with point sources, the first determination of the ultimate spectral resolution of the two grating sections of the SWS was done in space. The excellent results of the first in-orbit determination of spectral resolution, instrumental profiles and wavelength calibrations have already been reported by Valentijn et al. During the course of the mission the stability and reproducibility of the grating scanners have been measured on a routine basis as part of the calibration programme. As an example of the stability we show the results of a wavelength calibration from revolution 360 and 790 in Figure 2. Here the deviations in LVDT readings between the initial calibration table and actual calibration measurement are shown for the full range of scanner settings. The SW scanner values are shown in the top two curves, the LW scanner values are in the lower two curves. Calibration tables were updated when the difference was more than two LVDT units.

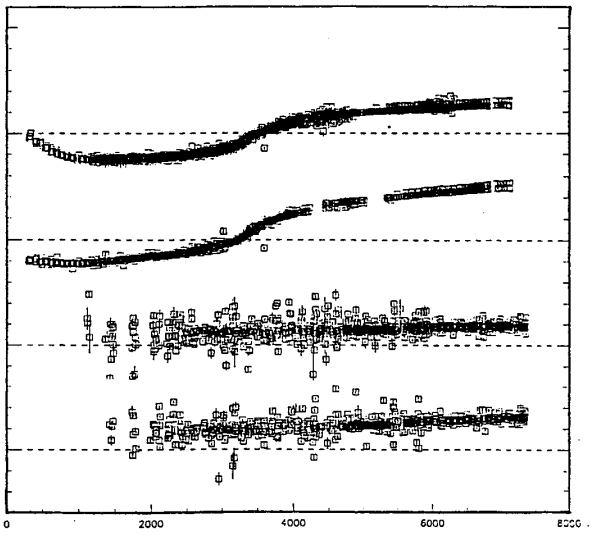

Figure 2. Deviations of the readout of the SW (top pair) and LW scanners (lower pair) from the values in the calibration tables for revolutions 370 and 670. Separations between the dotted lines are 5 LVDT units. One LVDT unit represents a wavelength shift of 0.01 to 0.02 %.

Also the Fabry-Perot turned out to be extremely stable and operated as was predicted from ground tests. Resolving power range from 25.000 to 30.000 for the 17 to 40 micron ranges and was checked against emission lines of external sources. The wavelength calibration carried out with the SWS internal calibrator and repeated with external sources was better than 1/3 of a resolution element. It is expected that the wavelength accuracy will improve somewhat by more line observations carried out in the routine observing programme.

One small problem, already suspected during ground calibration, was the misalignment of the Fabry-Perot channel through aperture 3 with the rest of the instrument. This turned out to be too large to be ignored. For this a fourth virtual aperture was defined and a change in AOT-07 was implemented.

The most dramatic difference between the laboratory tests and the in-orbit performance was the impact of the ionising radiation particles on the behaviour and performance of the SWS detectors. As already described in the previous section, due to the high frequency of impact occurrence, the integration reset time had to be restricted to 2 seconds for all bands except for band 1 where also 4 seconds could be used. Although the dark currents are more or less of the same magnitude, the dark noise is

several factors higher, except for band 1 where the difference is about 50%. The result is that the overall detector sensitivity was reduced with several factors for all detectors, except (again) for band 1. An overview of the average sensitivity loss for the detector bands is given in figure 1. The sensitivity ratio given here includes the effect of observing point sources in orbit against using extended sources in the laboratory. This effect may amount to 30 % in some cases. Dark currents and dark have been stable through the mission, except for band 3 with the Si:As BIBIB detectors.

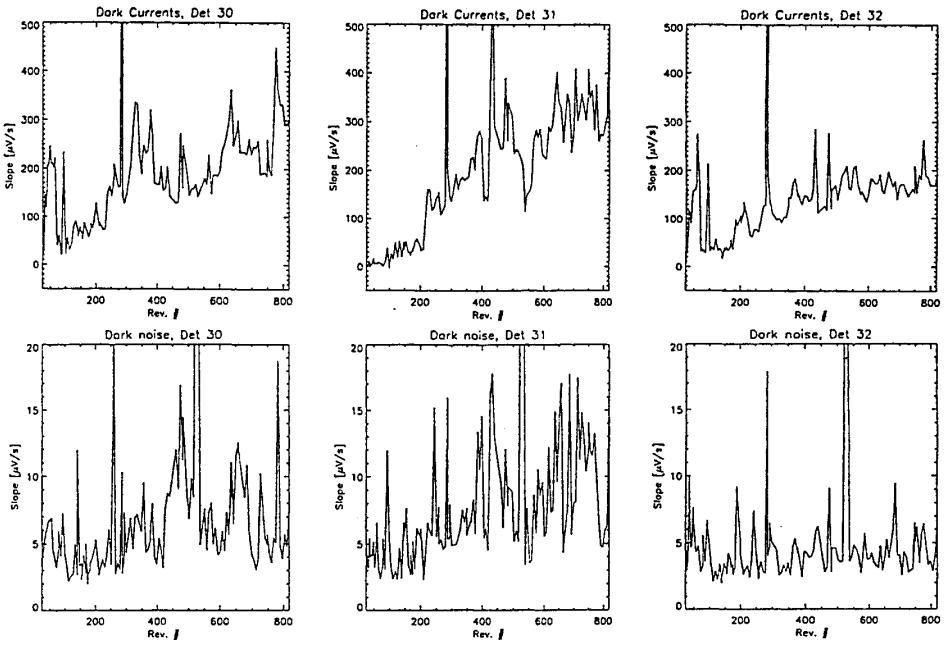

Figure 3. Dark current and noise for three Si:As BIBIB detectors as function of time in the mission.

Here is a clear increase in dark current with revolution as is shown in figure 4, in the top 3 panels. The lower 3 panels show the development of the dark noise with revolution number. Not all detectors show an increase in noise by revolution 800.

The detector responsivity as a function of time in the mission, is stable in all bands. This has been checked with the internal source and against many scans of astronomical sources with a wide range of spectral properties and fluxes. The accuracy is limited by the sensitivity and by short-term drifts and memory effects. The memory effects were negligible for bands 1 and 3; bands 2, 4, 5 and 6 have small to moderate memory effects.
Figure 5 shows for representative detectors of the four grating detector bands the dark currents, dark noise and response as a function of time into a revolution. The dark currents are higher in the beginning of the revolution, except for band 3, where the effect is less important. The detector response in band 2 is higher in the beginning of the revolution by 40%, whereas the effect for band 3 and 4 is below 10%.

5. RELATIVE SPECTRAL RESPONSE FUNCTION AND FLUX CALIBRATION

The relative spectral response function (RSRF) was initially measured in the lab with a blackbody source with temperatures between 30 and 300K. After launch, the RSRF was determined again but now using a range of standard stars and asteroids, with a special calibration up-link procedure where every scanner position was scanned. The RSRF was then obtained by dividing the measured spectrum by a model of the observed star. Extreme care has to taken in order not to introduce false features from inaccuracies in the model. The laboratory and the in-orbit RSRF were carefully compared. Differences between

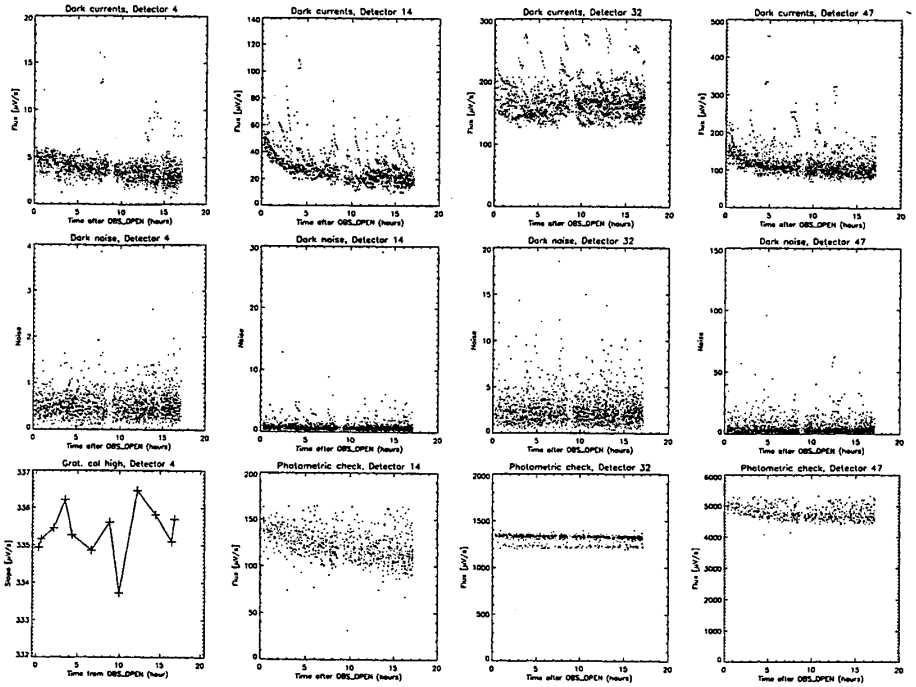

Figure 4. Dark currents, dark noise and reponsivity as function of time into the revolution shown for one detector per grating detector band.

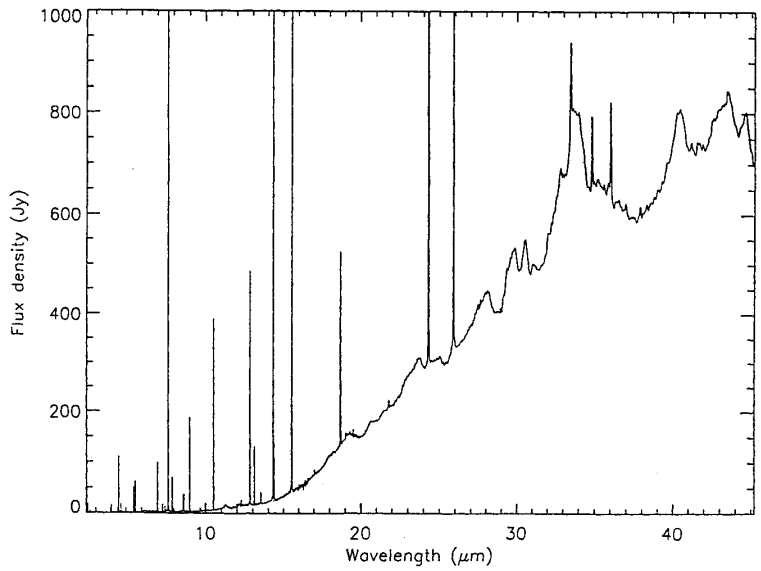

Figure 5. Complete SWS scan of the Planetary Nebula NGC 6302 showing strong narrow emission lines and wider features of crystalline silicates on top of a broad continuum.

the two are due to fringing effects, not only in band 3 where these effects had been observed in the laboratory tests, but also in bands 1 and 2. These fringing phenomena were stronger in orbit, because the ground tests were done with the equivalent of an extended source, whereas the in-orbit calibration uses point sources. These fill the entrance slits only partially and so increase the spectral resolution.
Also limitations in the temperature range of the laboratory blackbody source caused some of the differences, particularly for band 1. These effects, together with the uncertainties in the Spectral Energy Distribution of the calibration source, the short term drifts of the detector dark current, memory effects and inaccuracies in satellite pointing, limit the flux calibration accuracy. Nevertheless already good results have been obtained ranging from 5 to 30 % for bands 1 to 4. See table 1.
The reproducibility of the flux determinations obtained from repeated observations of the standard star HD6705 range from 1% for band 1 to a few % for the other bands. It turned out that inaccuracies in the pointing dominate the flux accuracy.
The flux calibration of the Fabry-Perot, which is tied to the one of the LW grating section, is of similar magnitude.

As a demonstration of the SWS performance a complete SWS spectrum of the Planetary Nebula NGC 6302, observed by Beintema et al, is shown in Figure 5.

6. ACKOWLEDEGEMENTS

ISO[5] is an ESA project with instruments funded by ESA Member States (especially the PI countries: France, Germany, the Netherlands and the United Kingdom) and with participation of ISAS and NASA. We are thankful to all the members of the ISO project at ESTEC, ESOC and Aerospatiale/MBB for their contributions, in particular H. Steinz, P. Lajous, H. Eggel and H. Schaap. The ground segment at Villafranca/Madrid (Vilspa) is acknowledged for their efforts preparing and running the ISO operations, in particular the ISO project scientist M. Kessler. We are greatly indebted to the hardware teams at Groningen and Garching for their effort in the development and construction of the SWS.

7. REFERENCES

[1]Th. de Graauw, L.N. Haser, D.A. Beintema, et al., " Observing with the ISO Short-Wavelength Spectrometer", *A&A,* **315**, pp L49-L54, 1996.
[2]K.J. Wildeman, W. Luinge, D.A. Beintema, et al., "Experiences with cryogenic short-wavelength spectrometer for Infrared Space Observatory", *Cryogenics*, **33**, pp 402-410, 1993.
[3]S.G. Schaeidt, P.W. Morris, A. Salama, et al., "The photometric calibration of the ISO Short Wavelength Spectrometer", *A&A*, **315**, pp L55-L59, 1996.
[4] E.A. Valentijn, H. Feuchtgruber, D.J.M. Kester, et al., *A&A*, **315**, pp L60-L63, 1996.
[5]M.F. Kessler, J.A. Steinz, M.E. Anderegg, et al., "The Infrared Space Observatory", *A&A*, **315**, pp L27-L31, 1996.